Palladium-copper membrane modules for hydrogen separation at elevated temperature and pressure

Dong-Kyu Moon*, Yun-Jin Han*, Gina Bang*, Jeong-Hoon Kim**, and Chang-Ha Lee*,†

*Department of Chemical and Biomolecular Engineering, Yonsei University, 50 Yonsei-ro, Seodaemun-gu, Seoul 03722, Korea
**Carbon Resources Institute, Korea Research Institute of Chemical Technology, 141 Gajeongro, Yuseong-gu, Daejeon 34114, Korea

Abstract–Two Pd-Cu alloy membrane modules were designed to recover high-purity hydrogen from a mixture at elevated temperature and pressure. Permeation and separation behavior were studied experimentally and theoretically using pure hydrogen gas and a binary mixture of H_2/CO_2 (58.2 : 41.8 in vol%) at 250-350 $^\circ$C and 800-1,200 kPa. The Pd-Cu membrane modules presented a maximum permeation flux at the highest temperature (350 $^\circ$C) and pressure (1,200 kPa) both for pure H_2 gas and the binary mixture. When the permeate and retentate flowed in the same direction in the membrane module (co-current flow), a temperature gradient and permeation flux variations were observed and the permeance of the H_2/CO_2 mixture was 2.263×10^{-4} mL/(cm$^2 \cdot$s$\cdot$Pa$^{0.5}$) at 250 $^\circ$C and 3.409×10^{-4} mL/(cm$^2 \cdot$s$\cdot$Pa$^{0.5}$) at 350 $^\circ$C. On the other hand, when the retentate flowed in the opposite direction to the permeate flow (counter-current flow), the temperature gradient and permeation flux variations were significantly reduced and the permeation flux improved by about 11% from that of the co-current flow module. The well-distributed temperature profile inside the module and increased hydrogen pressure difference through the membrane layer shortened the time to reach the steady state in the counter-current Pd-Cu membrane module, thus enhancing the membrane performance. The results of this study can contribute towards developing an efficient Pd-Cu membrane reactor.

Keywords: Pd-Cu Membrane, Hydrogen Separation, Hydrogen/Carbon Dioxide Mixture, Counter-current Flow Module

INTRODUCTION

Hydrogen has gained enormous attention as an alternative energy carrier or raw chemical for reactions. Using hydrogen as energy source may solve problems related to global climate change, energy security, and local air pollution. The steadily increasing demand for hydrogen has inspired many researchers to developed novel methods for hydrogen production, separation, and purification [1]. Especially, hydrogen separation and purification from a variety of sources is of specific importance for its application since the hydrogen produced by the chemical and petrochemical industries contains less desirable components (impurities) [2].

One of the approaches to produce hydrogen is via bulk separation and purification using a membrane module, which offers advantages of easy operation and high efficiency. Moreover, membrane separation technologies are an energy-efficient tool with the possibility of continuous operation without any phase transition during the process. As an alternative application, membrane reactors, combining reaction and separation, can offer numerous advantages for hydrogen production in next-generation chemical and power production systems [3]. Recent investigations on the synthesis, structure, and gas-transport properties of diverse membranes have been pursued to obtain membranes with good permeability, selectivity, and stability. In addition, in order to design membrane modules with high efficiency, the dynamic separation behavior and performance of membrane and hybrid membrane modules have also been studied in detail [4,5].

Since many applications require H_2 with high purity (including PEM; proton exchange membrane modules), membrane modules must offer effective routes to produce ultrapure hydrogen. Among various membrane materials for the separation of H_2 mixtures, dense metal membranes typically transport hydrogen in its dissociated form, providing a theoretically infinite selectivity [6]. Palladium membranes have received attention because of their excellent permeability and high durability against hydrocarbon streams [7]. Pd-based membranes present a solution-diffusion mechanism, consisting of adsorption of H_2 onto the metal surface, dissociation of H_2, diffusion of atomic H through dense metal and associative desorption of the H_2 from the metal surface, which is different from that of other inorganic membranes owing to its dense structure [8]. Hydrogen diffusion through the Pd lattice is fast due to high catalytic activity toward hydrogen dissociation into monoatomic hydrogen at metal surface compared to other metals [9].

Efficient membranes must display long lifetimes under operating conditions. However, pure palladium membranes have been reported not to meet this requirement because of embrittlement, poisoning, and degradation problems during H_2 separation at high temperature. To overcome these issues, current research focused on Pd alloyed with other metals, such as copper, silver, and gold. Among them, palladium copper (Pd-Cu) membrane has been wide-stud-

ied for hydrogen separation from various effluent gases because of their low cost of copper and their high resistance to sulfur poisoning compared to pure Pd and Pd-Ag membrane [10,11], showing higher permeability than pure palladium ones [12]. It has also been reported that ternary alloy membranes, where another metal is added to the Pd-Cu alloy membrane, is able to give enhanced H_2 separation performance [13].

Since the water-gas shift reaction (WGSR) after steam reforming processes using natural gas affords higher CO conversions at relatively low temperatures [14], application of hydrogen-selective Pd-Cu membranes for hydrogen separation is highly possible, allowing the integration of the WGSR process in a membrane reactor [15]. However, to achieve a Pd-Cu membrane design with high separation efficiency, the separation mechanism should be first elucidated under different operating conditions. Furthermore, well-designed membrane modules are required to maximize the separation efficiency, thus reducing the overall number of membrane modules in a given system.

The difference in the separation performance between the counter-current and co-current flow operation of a sweep gas relative to a feed flow in membrane processes has been discussed [16]. Recently, the concept of co- and counter-current flow model has been applied to a membrane reactor for effective hydrogen production, such as methanol steam reforming and WGSR reaction [17-21]. The results using a Pd-Ag membrane showed that the counter-current model gives higher membrane reactor performance than the co-current flow model with respect to hydrogen yield and recovery [18-20]. The previous studies mentioned used the concept of co- and counter-current flow between sweeping gas and retentate flow. As a result, the main concern was the effects of the sweep gas flow direction on the outside surface of a membrane. Few studies were conducted for the effects of the retentate gas flow direction on the inside surface of a membrane and separation performance. In the study, considering the co- and counter-current flow model between permeate and retentate flow without a sweeping gas, two Pd-Cu membrane modules were designed for H_2 separation from a binary mixture (H_2/CO_2=58.2 : 41.8 in vol%). To design efficient membrane reactor modules, it is important to understand the hydrogen permeation/separation characteristics of Pd-Cu membrane and the performance of its module. Therefore, the permeation and separation of pure H_2 and a H_2/CO_2 binary mixture were experimentally and theoretically investigated under unsteady and steady-state conditions. The experiments were carried out at 250-350 °C and 800-1,200 kPa (gauge pressure), considering the effluent gas conditions from WGSR processes. Then, two types of Pd-Cu membrane modules were designed and evaluated for effective hydrogen production: a co-current and a counter-current flow membrane module with respect to the permeate and retentate flows.

H₂ PERMEATION MODELING

To understand the hydrogen permeation behavior of the Pd-Cu membrane modules, mathematical models were developed on the basis of the following assumptions [22,23]: (i) the gas phase behaves as an ideal gas mixture, (ii) the palladium layer and metal mesh layer support are in thermal equilibrium, and (iii) the rate-limiting

step in the hydrogen transport mechanism is the unidirectional diffusion through the palladium layer.

In case of many membrane processes, the solution-diffusion mechanism is proposed as a permeation mechanism, which can be expressed well by using one-dimensional Fick's law. When gas solubility is independent of concentration, it can be expressed using Henry's law, where the driving force is the partial pressure difference over the membrane [24-26]. Since the specific properties of Pd-based membranes originate from a solution-diffusion mechanism and the rate-limiting step is the hydrogen transport mechanism through the palladium layer for hydrogen permeation, the overall molar flux (N_i) of component i can be described by a mass flux caused by hydrogen transport through the Pd-Cu membrane and defined as the rate of hydrogen passing through the membrane per unit area. The hydrogen flux is described by Eq. (1).

$$N_{H_2} = \pi \frac{(P_{H_2, feed}^{\,n} - P_{H_2, perm}^{\,n})}{x_m} \tag{1}$$

where N_{H_2} is the hydrogen flux, π is the hydrogen permeability coefficient, x_m is the membrane thickness and $P_{H_2, feed}$ and $P_{H_2, perm}$ are the partial pressure of hydrogen on the inside and permeation sides of the membrane, respectively.

If the diffusion of atomic hydrogen through the metal bulk of the membrane is the rate-determining step and the hydrogen concentration in the Pd-based lattice is sufficiently smaller than 1, Sieverts' law, which has traditionally been suggested for modeling the H_2 permeation flux in metallic membranes, can be applied [27]. The value of the exponent n in Eq. (1) is related to the transport step controlling the hydrogen flux [28-30]. An n-value of 0.5 implies that transport is controlled by the diffusion step, while an n-value of 1 implies that transport is controlled by the surface adsorption step. For membranes with a thickness of over 15 μm, it has been reported that the n-value tends to be ~0.5 [22,26].

In this study, the surface adsorption was considered to be very fast. Therefore, the rate-limiting step would be the atomic hydrogen diffusion through the metal lattice. Consequently, the hydrogen flux through a thick palladium membrane (>15 μm) could be proportional to the difference in the square root of the hydrogen pressure on either side of the palladium alloy, in accordance with Sieverts' law. An n-value of 0.5 was thus applied to Eq. (1):

$$N_{H_2} = \pi \frac{(P_{H_2, feed}^{\,0.5} - P_{H_2, perm}^{\,0.5})}{x_m} \tag{2}$$

The gPROMS® process builder (Process Systems Enterprise Limited, UK) was used to obtain the permeation flux from the above mathematical model. A second-order centered finite difference method (CFDM) was applied to the spatial partial derivatives. Differential-algebraic equations (DAEs) for the temporal domain were subsequently integrated employing an integrator called DASOLV in the gPROMS library [31].

EXPERIMENTAL SECTION

1. Design of the Experimental System with a Pd-Cu Membrane Module

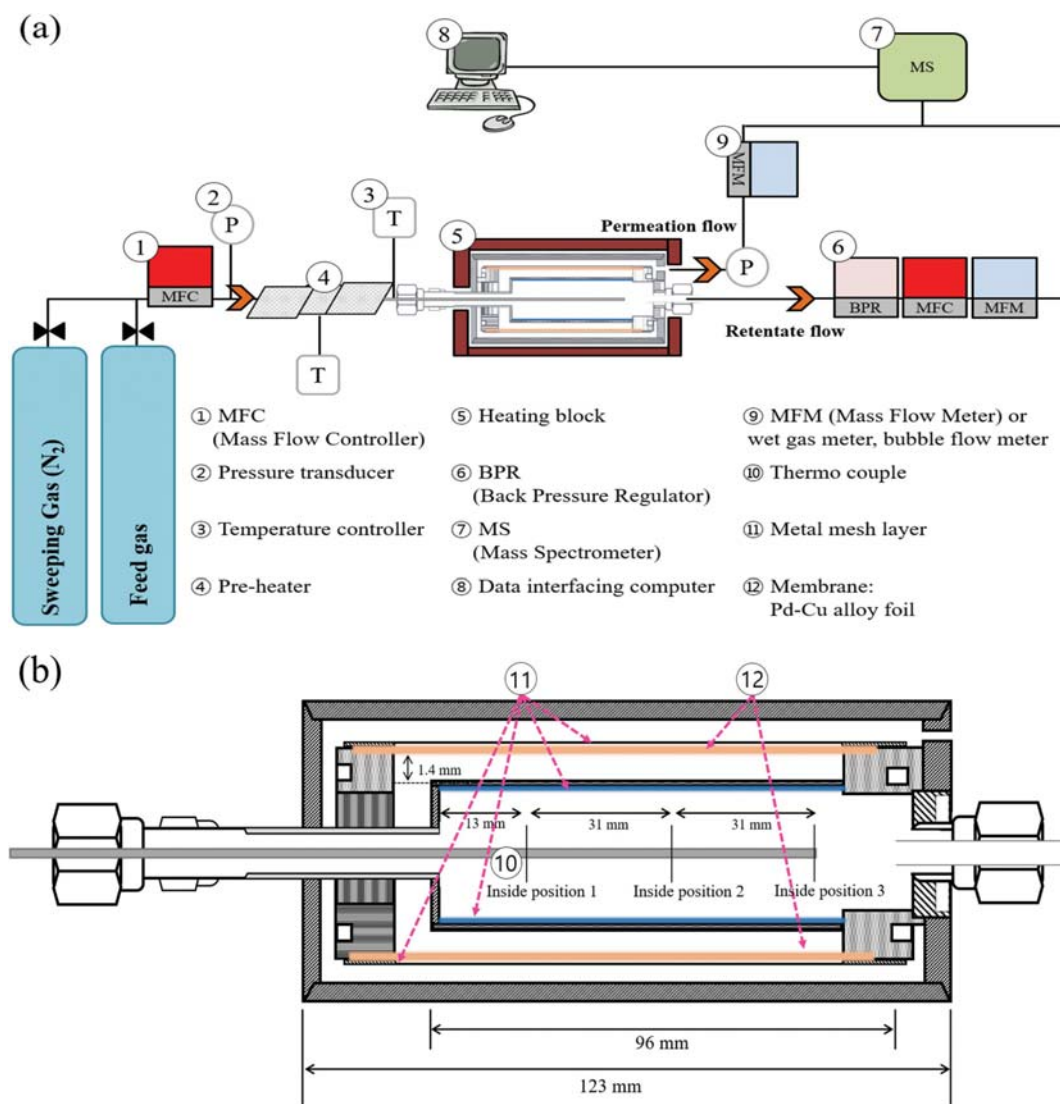A schematic of the membrane system with the Pd-Cu mem-

Fig. 1. Schematics of the experimental membrane (a) system and (b) module.

brane module used in this study is shown in Fig. 1(a). The membrane module was fitted with a feed gas inlet line, a retentate flow outlet, and a permeate flow line. The membrane module was located in a heating block, and the gas inlet line was equipped with a pre-heater (electric heating tape) controlled by two temperature controllers (Eurotherm Co., USA). The feed-gas flow was controlled by a mass flow controller (MFC, Tylan Co., USA) and a gas cylinder pressure regulator (Harris Co., USA). The retentate gas was controlled and maintained by another MFC and a back-pressure regulator (BPR, Bronkhorst high-tech, Netherland). Depending on the gas, a mass flow meter (MFM, Hastings Ins. USA), a soap bubble flow meter (Supelco Co., USA), and a wet gas meter (Sinagawa Co., Japan) were used to measure the flow rates of the permeate and retentate gases. Two pressure transducers (Sensyst Co., USA), calibrated by a pressure gauge (HEISE Co., USA), were placed at the gas inlet and permeate ports of the membrane module. The composition of the gas separated from the binary mixture was analyzed on an on-line mass spectrometer (QMG 422, Balzers Co.,

Table 1. Characteristics of the Pd-Cu membrane

Active area of membrane [m^2]	0.007
Thickness of the Pd-Cu alloy foil, x_m [m]	2.0×10^{-5}
Thickness of metal mesh layer [m]	1.0×10^{-5}
Max. pressure condition [MPa]	2.2
The length of the membrane [m]	9.6×10^{-2}
Inner diameter of the membrane [m]	3.0×10^{-2}
Copper concentration in alloy [wt%]	40

Germany). Before each experiment, the membrane system was heat-treated at 250 °C with N_2 flow for over 100 min to remove any contaminants.

The design and specifications of the membrane module are presented in Fig. 1(b) and Table 1. The Pd-Cu membrane with the active area of 0.007 m^2 was placed in a stainless steel tubular module. Both ends of the thin Pd-Cu membrane containing 40 wt% Cu with a thickness of 20 μm (NASLON Co., Japan) were held by
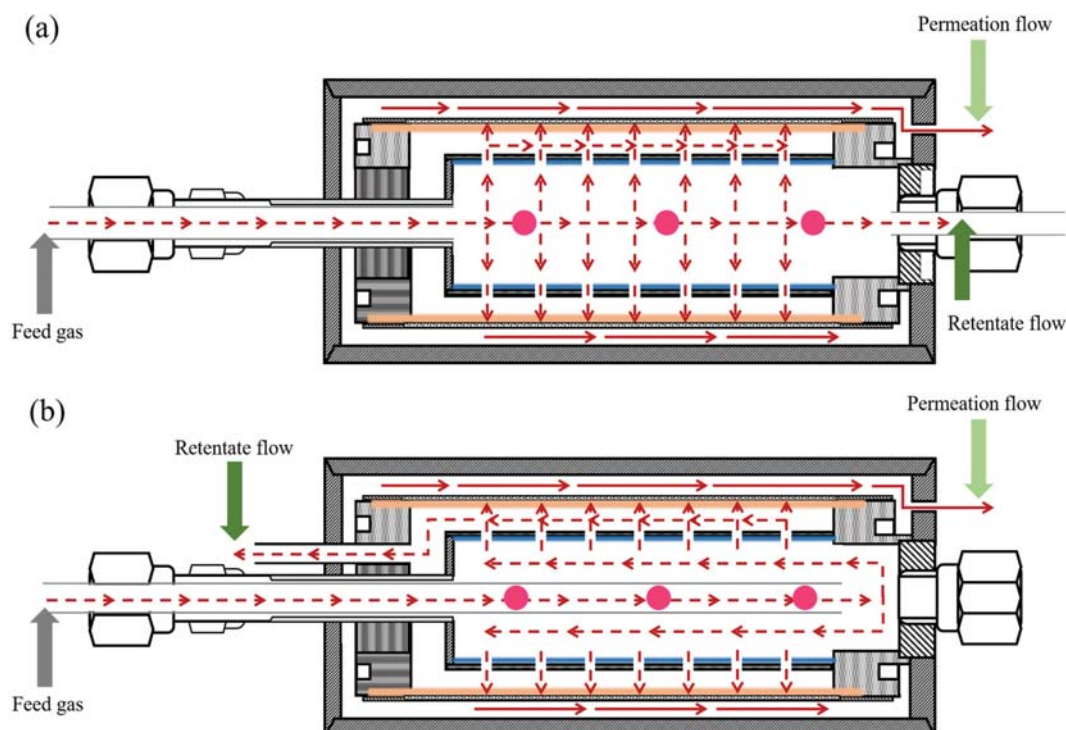
Fig. 2. Conceptual gas flow diagrams: (a) Co-current flow module and (b) counter-current flow module. The red dots indicate the position of the thermocouples.

a tubular nonporous asymmetric support. For chemical and mechanical stability, a metal mesh layer was inserted inside the membrane layer, acting as a filter able to maintain the membrane layer free from contaminants such as gas dust and powder. In addition, the membrane was supported by another metal mesh layer to prevent any damage from a high permeate flow or pressure difference, as shown in Fig. 1. When the module is used as a membrane reactor, a metal mesh filter layer can also work as a protector from powder which can be generated by catalysts. The material of a mesh filter is stainless steel type 316L (the pore size: 10 micron) and the porosity is 36 vol%. There was no direct contact between the Pd-Cu membrane film and the mesh filter layer. To measure the internal temperatures at three different positions of the membrane module, a three-position thermocouple (RTD type, Pt 100 Ω) passing through the gas inlet line was employed. All the thermocouples were centered radially in the module. The three thermocouples were axially located in front of the gas inlet, in front of the retentate gas outlet and in the center of the membrane module, respectively. The temperatures of the three positions were measured on a real-time basis, and the inside temperatures were labeled as Temp. (1), (2), and (3), located at 13, 44, and 75 cm from the feed-end of the membrane (Fig. 1(b)). The membrane module designed by our group was manufactured by NASLON Co., Japan.

2. Design of the Pd-Cu Membrane Modules

The Pd-Cu membrane should theoretically exhibit infinite hydrogen selectivity. However, due to the dense structure of the membrane, it is not easy to obtain adequate permeation fluxes during gas separation processes. Therefore, the t design of effective membrane modules to allow for efficient permeation performances is crucial. However, no sweep gas was employed on the Pd-Cu membrane modules in this study. Since the direction of sweep gas in membrane modules is generally the same as the direction of permeate gas, the flow pattern of Pd-Cu membrane modules was defined by the same concept as the sweep gas in a general membrane operation.

In this study, two membrane modules with different flow patterns with respect to the permeate and retentate flows were designed (Fig. 2). As shown in Fig. 2(a), the gas from the feed inlet to the retentate outlet flowed co-currently to the permeation flow direction, which is called the co-current flow module. When the feed inlet line was extended to the end of the membrane module and the retentate outlet line was located at the same position as the feed inlet line, it was called the counter-current flow membrane module (Fig. 2(b)). Therefore, the direction of retentate flow is opposite to that of the permeate flow. Furthermore, in the counter-current flow module, the feed is expected to reach the operation temperature easily by heat exchange in the pass-through feed line. In addition, the CO_2 concentration polarization on the membrane surface may be reduced by the flow in the space (1.4 mm) between the Pd-Cu foil and the metal mesh support.

3. Permeation Experiments

The experimental permeation measurements in the Pd-Cu membrane module were conducted in the temperature range of 250-350 °C and pressure range of 800-1,200 kPa (gauge pressure) without any sweeping gas. The permeated gas was vented out from the module at atmospheric pressure. Prior to the main permeation experiments, the activation of membrane and the leakage test of the membrane module were carried out by N_2 at 1,500 kPa and 350 °C. It was confirmed that no substance was detected by the

mass spectrometer on the permeate side.

The permeation experiments using pure H_2 (99.999 mol%) were under fixed retentate flow conditions (200 sccm: 200 standard cubic centimeters per minute) without sweeping gas since the retentate flux in the membrane is too small to affect the permeation flux of hydrogen gas.

A binary mixture of H_2 and CO_2 (58.2 : 41.8 vol%) was used as the mixed feed on the basis that the effluent gas of WGSR processes from methane-steam reforming units generally contains approximately 55-60 vol% H_2. The separation and permeation performance in the co-current flow membrane module was primarily investigated to elucidate the separation characteristics of the Pd-Cu membrane, and the unsteady- and steady-state results were compared to the separation performance of the counter-current flow membrane module. The permeation was measured at a fixed retentate flow (2,000 sccm) without sweeping gas, and the CO_2 concentration at the retentate outlet was measured with the varying retentate flow. The permeation of the binary mixture gas was also conducted at the temperature range of 250-350 °C and the pressure range of 800-1,200 kPa, which are similar to the effluent conditions of two-stage WGSR processes. Since the retentate flow rate was fixed by BPR and MFC, the feed flow rate was re-adjusted during the experiments. Because the membrane module performance and the feed flow can be affected by temperature, the membrane module temperature was carefully controlled by both a heating block and a pre-heater.

Transient permeation experiments (pressurization: atmospheric pressure→desired feed pressure) were also performed to analyze the permeation mechanism. The permeation flow rate was automatically adjusted through a back pressure regulator (BPR in Fig. 1) at a fixed retentate flow condition. And the permeation flux was directly measured by a mass flow meter and indirectly confirmed by an on-line mass spectrometer.

RESULTS AND DISCUSSION

1. Hydrogen Permeation through the Pd-Cu Membrane

Hydrogen of 99.999 mol% purity was used as the feed gas to investigate the pure hydrogen permeation properties of the Pd-Cu membrane. Permeation experiments were conducted by changing the temperature and pressure conditions at a fixed retentate flow rate (200 sccm).

Fig. 3 shows the transient permeation (pressurization step) of H_2 on the co-current flow membrane module shown in Fig. 2(a) at 350 °C and 1,000 kPa. The transient hydrogen permeation flux curve mostly exhibited a sharp increase for about 300 s. During this period, the permeation flux reached over 95% of the steady-state flux value (approximately 1.0 mL/cm^2 s). Then, the permeation flux gradually approached the steady-state flux. The temperature inside the co-current membrane module was lower than the experimental temperature up to 2,000 s, showing a maximum of 10 °C difference at the feed end (Temp. (1) in Fig. 3). This suggested that a homogeneous temperature in the co-current Pd-Cu membrane module was reached slowly. In addition, the shapes of temperature profiles and transient permeation flux in the counter-current membrane module were almost the same because of very low heat capacity of H_2 and the same heat transfer in the module as the co-current flow module. The difference in separation performance of mixture between two modules will be discussed in detail later.

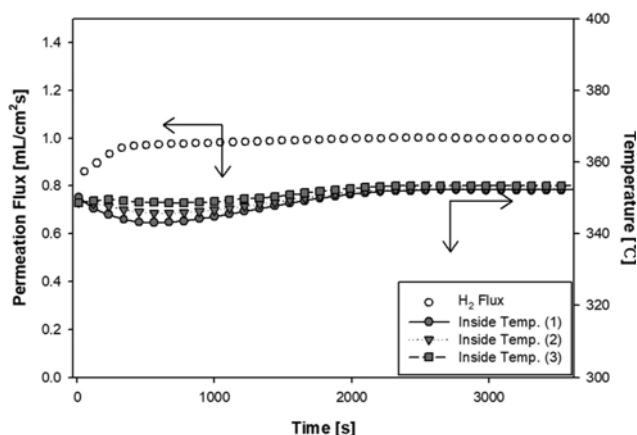The permeation flux increased with the pressure at a fixed tem-

Fig. 3. Transient permeation flux and temperature profiles of H_2 on the co-current flow Pd-Cu membrane module at 350 °C, 1,000 kPa and a retentate gas flow rate of 200 sccm.
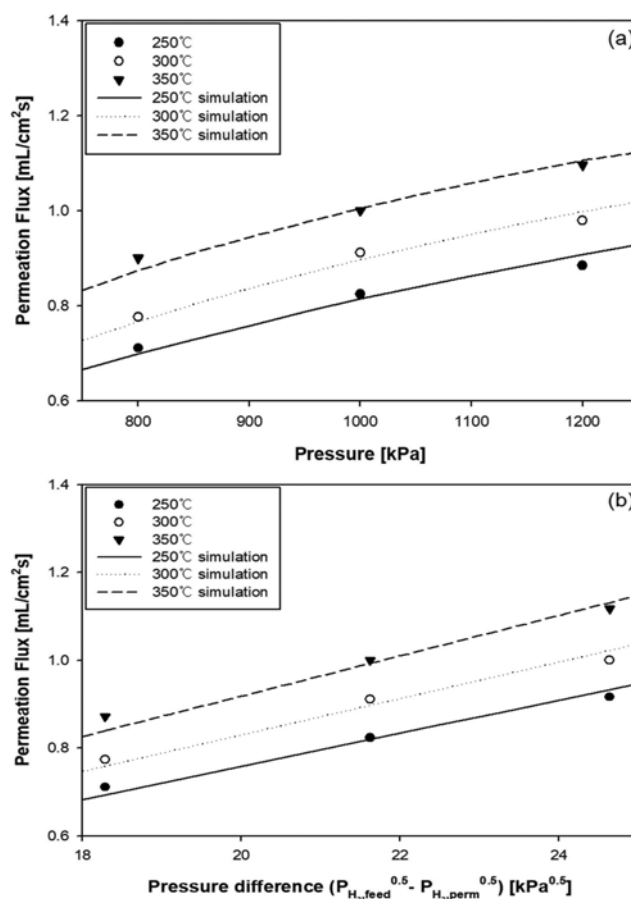

Fig. 4. Steady-state permeation flux of H_2 on the co-current flow Pd-Cu membrane module at 250-350 °C, 800-1,200 kPa (gauge pressure), and a retentate gas flow rate of 200 sccm: (a) Feed pressure and (b) pressure differences.

Table 2. Permeance of H$_2$ and the H$_2$/CO$_2$ mixture on the co-current flow membrane system at 250-350 °C

	H$_2$ $\times10^{-3}$ [mL/(cm^2·s·Pa$^{0.5}$)]			H$_2$/CO$_2$ $\times10^{-4}$ [mL/(cm^2·s·Pa$^{0.5}$)]	
	250 °C	300 °C	350 °C	250 °C	350 °C
This study (40 wt% Cu)	1.206	1.319	1.451	2.263	3.409
Reference [33] (40 wt% Cu)	1.120	1.458	1.633	-	-

perature, displaying a smooth curvature in Fig. 4(a). Under fixed pressure conditions, the permeation flux increased with the temperature. An improvement of ~0.2 mL/cm^2 in the permeation flux was obtained upon increasing the pressure from 800 to 1,200 kPa or the temperature from 250 to 350 °C. This indicates that the effect of a 200 kPa difference on the permeation flux is equivalent to the effect of a 50 °C difference. The permeance of H$_2$ on the co-current flow membrane system at each temperature is listed in Table 1, which ranges from 1.206 to 1.451×10^{-3} [mL/cm^2·s·Pa$^{0.5}$)]. The activated energy calculated from the permeability was 4.99 kJ/mol.
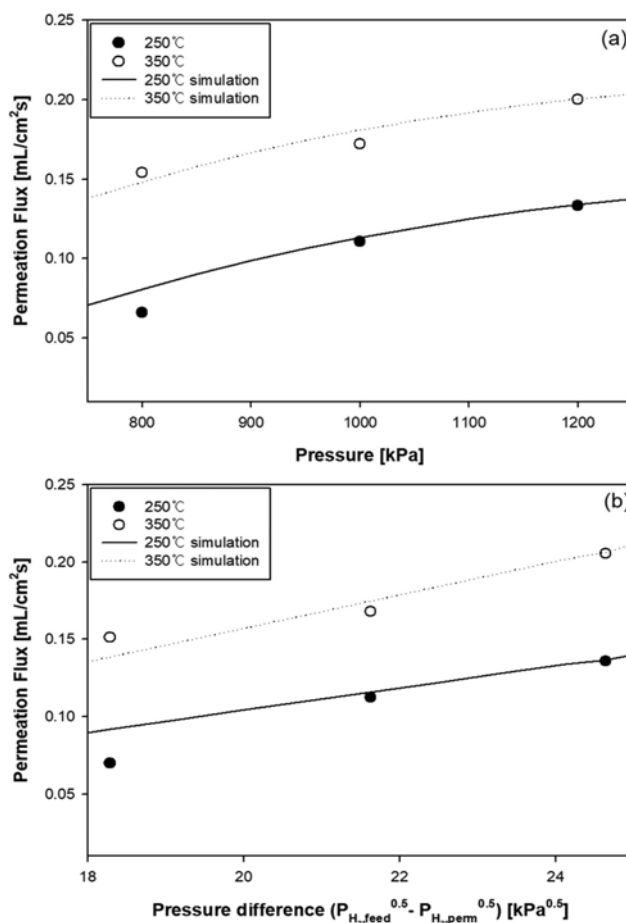
As described in the mathematical model section, Sieverts' law for hydrogen diffusion through the membrane layer was applied for single gas permeation through the Pd-Cu membrane. Assuming a constant temperature in the membrane, the steady-state permeation flux variation is proportional to the difference in the square root of the hydrogen pressure on either side of the Pd-Cu membrane (Fig. 4(b)). The temperature fluctuations in Fig. 3 are slightly larger at high temperatures, but they do not have a significant effect on the permeation flux of pure H$_2$. The permeance of H$_2$ increased with temperature, and the results reasonably agreed with a reference [33] as shown in Table 2.

2. H$_2$/CO$_2$ Separation with the Pd-Cu Membrane

2-1. H$_2$/CO$_2$ Permeation and Separation

The permeation flux for H$_2$/CO$_2$ (58.2 : 41.8 vol%) also increased with the feed pressure (Fig. 5). Owing to the adsorption and surface diffusion of CO$_2$ on the membrane surface, the permeation flux of H$_2$ in the binary mixture decayed 5-10 times, even at 2,000 sccm, compared to the case of pure hydrogen (Fig. 4). The permeation flux reached a steady state, like Fig. 3. The H$_2$ concentration of permeate flow at the steady state was almost pure; the results at the steady state were applied to Seiverts' model (Eq. (2)) in Figs. 4 and 5. Since both surface diffusion and adsorption occur rapidly, the adsorption and association step can be assumed to proceed almost simultaneously. However, the H$_2$ flux is significantly hindered by CO$_2$ molecules occupying the adsorption sites on the membrane surface. Since the adsorption affinity of the membrane toward CO$_2$ is stronger at lower temperatures, the reduction in the permeation flux was greater at 250 °C than at 350 °C. Furthermore, such reduction was most significant at the lowest temperature and pressure conditions (250 °C and 800 kPa). With the increasing pressure from 800 kPa to 1,200 kPa at 250 °C, the permeation flux increased from 0.0699 mL/(cm^2 s) to 0.1358 mL/(cm^2 s).

The Sieverts' model was able to predict reasonably the permeation flux of the binary mixture, as shown in Fig. 5. In case of pure H$_2$ experiments, the permeation flux depended almost linearly on the H$_2$ partial pressure difference. On the other hand, the permeation flux of the binary mixture with a variation of H$_2$ partial pres-

Fig. 5. Steady-state permeation flux of H$_2$/CO$_2$ (58.2 : 41.8 vol%) on the co-current flow Pd-Cu membrane at 250-350 °C, 800-1,200 kPa (gauge pressure) and a retentate gas flow rate of 2,000 sccm: (a) Feed pressure and (b) pressure difference.

sure difference showed somewhat curvature as shown in Fig. 5(a). When Sieverts' law was applied to the results, the permeation flux of H$_2$/CO$_2$ mixture became linearly proportional to the difference in the square root of hydrogen pressure on either side of the Pd-Cu membrane film in Fig. 5(b).

The hydrogen permeability coefficient ($\pi\times10^{-5}$ mL/(cm s kPa$^{0.5}$)) in Sieverts' law was determined as 7.59 (250 °C), 8.34 (300 °C), and 9.18 (350 °C) in Fig. 4(b). However, the deviation between the permeation flux results in experiments and simulation was somewhat higher than that in the pure H$_2$ permeation, especially at the lowest temperature and pressure difference. Upon applying higher π values (7.79×10^{-5} mL/(cm s kPa$^{0.5}$)) at 250 °C and 11.72×10^{-5} mL/(cm s

predict experimental results with the minimum error of permeation flux in Fig. 5(b).

The permeance results for the binary mixture were 2.263×10^{-4} mL/(cm²·s·Pa[0.5]) at 250 °C and 3.409×10^{-4} mL/(cm²·s·Pa[0.5]) at 350 °C. The permeance variation with the experimental conditions was different from that with pure H_2 with reference values [33], as shown in Table 2. The permeance of pure H_2 tended to increase almost linearly with temperature. In addition, the permeance of the binary mixture also increased as the temperature increased from 250 °C to 350 °C. However, compared to pure H_2, the increase in permeation was much greater when the temperature rose from 250 °C to 350 °C. It is expected that, at higher temperatures, smaller amounts of CO_2 are adsorbed on the membrane and CO_2 molecules move rapidly on the membrane surface. In addition, the membrane surface may be almost saturated with CO_2 molecules as pressure increases. However, since permeance is independent of pressure, it is only affected by temperature.

The reduction of the H_2 permeation may result from polarization of the CO_2 concentration. This effect at the membrane surface can be reduced by controlling the retentate flow rate so as to raise the H_2 partial pressure on the feed side of the membrane. Generally, the decreased flow rate of permeate was applied to reduce concentration polarization. However, in the study, since the permeate flow rate was controlled by a BPR at a fixed retentate flow condition as mentioned in the experimental section, the retentate flow rate was changed and it led to reducing the ratio of permeate flow rate to retentate flow rate. To confirm the effect of the retentate flow rate on the separation, the permeation flux and retentate composition were determined at 250 °C and 1,000 kPa with the increasing retentate flow from 500 to 2,000 sccm.

In Fig. 6, the permeation flux shows a linear increase because the desorption of CO_2 on the membrane surface improves with the increasing retentate flow. However, the H_2 concentration on the retentate flow also increases with the increasing flow rate. In addition, regarding the concentrated CO_2 in the retentate flow, the application of lower retentate flow rates to the Pd-Cu membrane is more desirable in general. Consequently, since the permeation flux is lower
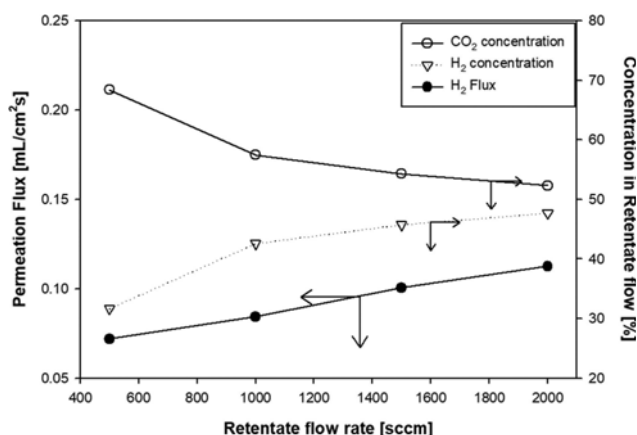

Fig. 7. Transient permeation flux and temperature profiles of the co-current flow Pd-Cu membrane for H_2/CO_2 (58.2 : 41.8 vol%) separation at 350 °C, 1,000 kPa and a retentate gas flow rate of 2,000 sccm.

at lower retentate flow rates, a suitable design of the membrane module is desirable so as to improve the permeation flux.

In this study, after a certain period of time during the permeation experiments with the H_2/CO_2 mixture, a drastic drop in the temperature and permeation flux was sometimes observed under the experimental conditions of 350 °C and 1,200 kPa, as shown in Fig. 7. In the experiments, the outside temperature of the membrane module was set to be higher than the experimental temperature. Due to difficulties in the temperature control of the permeation and retentate flows, the inside and outside temperatures were sometimes higher than the desired temperatures, as shown in Fig. 7.

In this figure, the permeation flux and the inside temperature decreased significantly after ~1700 s with the presence of water, acting to deteriorate the performance of the membrane film, from inside the module to the retentate outlet flow. Simultaneously, the outside temperature of the membrane module was gradually increased to control the inner temperature. The endothermic reaction and high heat capacity of water molecules led to significant temperature reduction regardless of the increasing outside temperature.

A few studies have reported the uncatalyzed RWGS reaction (an endothermic reaction) at high temperatures (>400 °C) under different pressure conditions [35,36]. In addition, exposure to CO can deposit carbon and form CO_2 on the membrane film by the reverse reaction ($2CO \rightarrow C(s)+CO_2$), which means that there occurs the carbon deposition and the retarding effect of CO_2 on the Pd-Cu alloy membrane [37-39]. In the experiment, the internal temperature increased slowly with time at the initial temperature of 350 °C. After a certain period of time, the H_2 permeation flux was rapidly decreased, showing a certain amount of water from the outside port of the membrane. Furthermore, when significant reduction of the permeation flux occurred, the separation performance of the Pd-Cu membrane could not be recovered by inert gas flow treatment at high temperatures (N_2 flow at 250 °C for over 100 min and H_2 flow at 250 °C for 30 min).

In this work, a temperature gradient inside the membrane modules (differences in local temperatures) was observed even though the temperature variation was small. Therefore, the Pd-Cu mem-

Fig. 6. Concentration of H_2/CO_2 in the retentate flow for the co-current flow Pd-Cu membrane module at 250 °C, 1,000 kPa and retentate gas flow rates of 500-2,000 sccm.
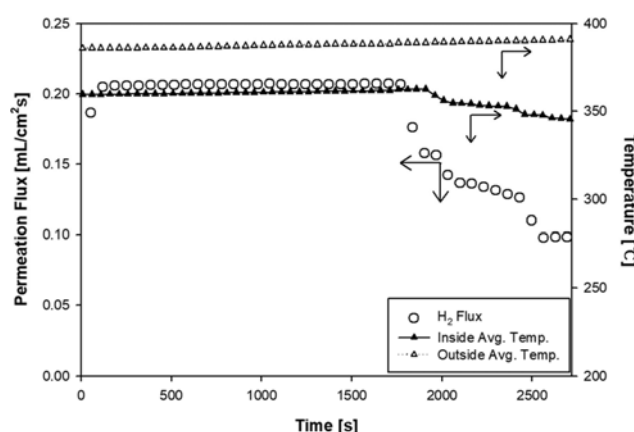
brane should be carefully operated at 350 °C, and the temperature control in the membrane module is critical to maintaining performance. Furthermore, well-designed membrane modules are important to reduce the inner temperature gradient and achieve high membrane separation performance and stability.

2-2. Comparison of the Separation Performance of the Two Different Flow Modules

As presented in Fig. 2, a counter-current flow membrane module was designed in this study to improve the separation performance. The experimental transient permeation flux and temperature profiles for H_2/CO_2 separation in the co- and counter-current flow membrane modules are presented in Fig. 8.

In the co-current flow membrane module, the temperature reaches steady-state conditions after 4,000 s. Furthermore, temperature fluctuations at the feed end are significant, and a temperature gradient in the membrane module is clearly observed in Fig. 8(a). Even though the average temperature is ~250 °C, a homogeneous temperature inside the membrane module is not reached until >5,000 s. In contrast, the permeation flux reached the steady state at 4,000 s, showing a ca. 10 °C difference in the module between the thermocouple positions. The temperature of the membrane surface should be >260 °C due to the outside module heater.

In Fig. 8(a), the permeation flux is low at temperatures lower than the desired value. It took a longer time to reach the steady state compared to the results for pure H_2 (Fig. 3). These phenomena can be expected at high feed flow rates (2,000 sccm in the study) and

feeds containing molecules with high heat capacities. Furthermore, when applying high temperatures to the Pd-Cu membrane to increase its separation performance, the temperature differences at different positions of the membrane must be carefully monitored in this co-current membrane module because unexpected high temperatures at certain local sites may lead to the RWGS reaction, as described above.

In this study, the purpose of designing a counter-current flow membrane module was to improve the inside temperature control and reduce the concentration polarization. In the counter-current membrane, a feed line was inserted in the membrane module for heat exchange between the feed flow and membrane module. In addition, to reduce the CO_2 concentration polarization on the membrane surface, the retentate flowed counter-currently to the direction of the permeate flow, as shown in Fig. 2(b). Therefore, even though the CO_2 concentration increases along the Pd-Cu membrane between the membrane and porous supporter, the feed is in continuous contact with the membrane throughout the module.

As shown in Fig. 8(b), the temperature fluctuation and gradients in the counter-current system are significantly reduced compared to those of the co-current flow membrane module in Fig. 8(a). Therefore, the permeation flux and temperature reach the steady-state conditions very quickly. In the developed counter-current flow membrane module, the temperature control in the module is achieved easily by a preheating effect through the inserted feed line. Note that the transient permeation flux and temperature profile in the co-current system using pure H_2 in Fig. 3 are more similar to those of the counter-current system in Fig. 8(b) than the co-current system in Fig. 8(a). Due to relatively high heat capacity of CO_2, larger heat transfer area in the counter-current system contributes to well-developed temperature distribution in the counter-current system. Furthermore, since almost the same temperature is applied to the whole membrane surface at the steady state (~2,500 s in the experiment), the temperature control required to avoid the RWGS reaction in local hotspots is successfully achieved.
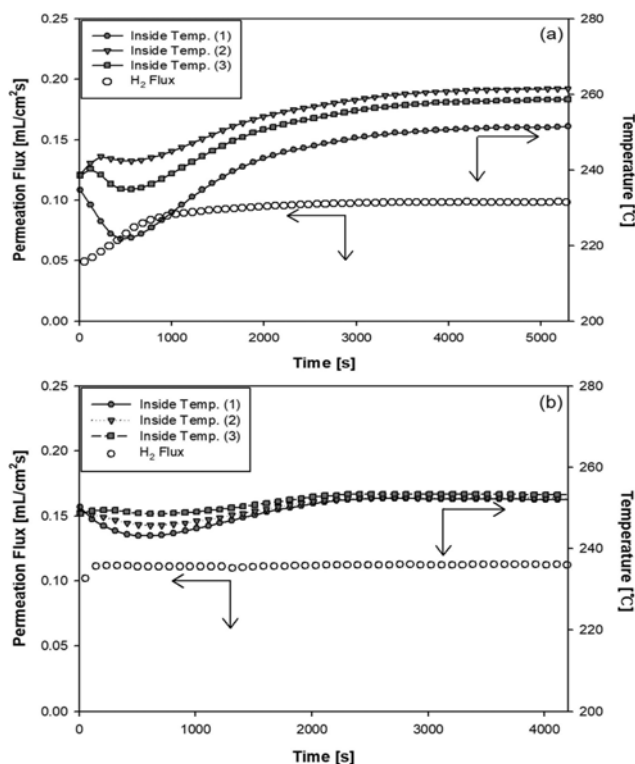

Fig. 8. Transient permeation flux and temperature profiles at different positions of the (a) co-current flow and (b) counter-current Pd-Cu membrane module for H_2/CO_2 separation at 250 °C, 1,200 kPa and a retentate gas flow rate of 2,000 sccm.
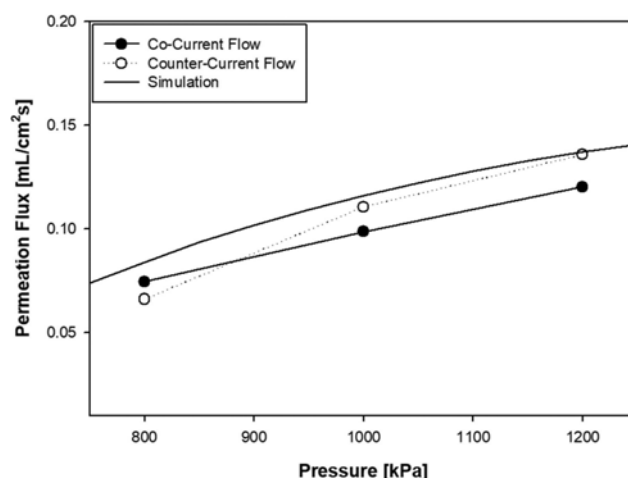

Fig. 9. Comparison of the permeation flux of H_2/CO_2 (58.2 : 41.8 vol%) in co-current and counter-current flow Pd-Cu membrane modules at 250 °C, 800-1,200 kPa (gauge pressure) and a retentate gas flow rate of 2,000 sccm.

Fig. 9 shows a comparison of the permeation flux between the co-current and counter-current flow membrane modules under the same temperature and retentate flow rate. The permeation flux of the counter-current flow membrane module was improved by about 11% from that of the co-current flow membrane module. However, the higher permeation flux at 800 kPa resulted from larger temperature differences in the membrane module. As mentioned, the separation might be carried out at temperatures higher than the set temperature because temperature control is more difficult under low pressure conditions. Furthermore, in the counter-current flow membrane module, steady state is reached faster, saving time. The advantages of such a counter-current flow membrane module become more prominent at higher pressures because the reduction of the temperature gradient and CO_2 concentration polarization are greater under denser gas conditions.

CONCLUSIONS

The permeation characteristics and separation behavior of a Pd-Cu membrane toward the production of high purity H_2 were studied experimentally and theoretically using pure H_2 and a binary mixture ($H_2/CO_2=58.2:41.8$ vol%). Considering the effluent gas conditions from typical low-temperature WGSR units, the experiments were carried out at 250-350 °C and 800-1,200 kPa. The H_2 concentration of the permeation flow in the Pd-Cu film was 100% H_2, which is why the metal membrane was used for hydrogen separation from hydrogen mixture in the many membrane processes. Hereby, separation factor and/or recovery did not have to be discussed in this study.

The permeation flux of pure H_2 was linearly proportional to the difference of the square root of the pressure. In the co-current flow membrane module, the maximum permeation flux of H_2 was 1.116 mL/(cm^2 s) at 350 °C and 1,200 kPa. The permeance results for the binary mixture were 2.263×10^{-4} mL/(cm^2·s·Pa$^{0.5}$) at 250 °C and 3.409×10^{-4} mL/(cm^2·s·Pa$^{0.5}$) at 350 °C. The maximum permeation flux was 0.2056 mL/(cm^2 s) at 350 °C and 1,200 kPa, and the maximum permeance was 3.409×10^{-4} mL/(cm^2·s·Pa$^{0.5}$) at 350 °C. A mathematical model based on Sieverts' law was able to accurately predict the experimental permeation fluxes of pure H_2, as well as those of the binary mixture reasonably.

In the co-current flow membrane module for the mixture separation, the permeation flux was improved by increasing the retentate flow rate, thus reducing the CO_2 concentration polarization effect on the membrane surface. However, the H_2 concentration in the retentate outlet flow increased with the retentate flow rate, and the ability of the membrane to concentrate CO_2 from the feed was significantly reduced. In addition, temperature control was found to be key in this system due to the existence of temperature gradients and fluctuations in the module. Furthermore, the RWGS reaction was observed at 350 °C and 1,200 kPa, which led to a significant reduction of the permeation flux and membrane contamination. Therefore, the temperature distribution should be carefully controlled in such co-current flow Pd-Cu membrane modules.

To overcome such temperature gradients, fluctuations, and CO_2 concentration polarization in the membrane module, a counter-current flow membrane module with an inserted feed line was developed. The developed module enabled the significant reduction of the temperature gradient and fluctuations by a preheating effect and changing the feed-flow direction. Due to these advantages, the time to reach the steady state was almost half that in the co-current flow membrane module. Furthermore, the permeation flux was increased by ~11% compared to that in the co-current flow membrane module. The suggested counter-current flow membrane module is expected to afford membranes with higher efficiency and greater thermal stability under high pressure conditions. Thus, the results of this study will contribute to designing an efficient Pd-Cu membrane reactor and operating membrane systems in the future.

ACKNOWLEDGEMENTS

REFERENCES

1. S. Adhikari and S. Fernando, *Ind. Eng. Chem. Res.*, **45**, 875 (2006).
2. W. Hu, X. Wu, Z. Li and J. Yang, *Phys. Chem. Chem. Phys.*, **15**, 5753 (2013).
3. M. D. Dolan, *J. Membr. Sci.*, **362**, 12 (2010).
4. Y.-J. Han, J.-H. Kang, H.-E. Kim, J.-H. Moon, C.-H. Cho and C.-H. Lee, *Ind. Eng. Chem. Res.*, **56**, 2582 (2017).
5. Y.-J. Han, K.-J. Ko, H.-K. Choi, J.-H. Moon and C.-H. Lee, *Sep. Purif. Technol.*, **182**, 151 (2017).
6. S. K. Gade, P. M. Thoen and J. D. Way, *J. Membr. Sci.*, **316**, 112 (2008).
7. M. Rahimpour, F. Samimi, A. Babapoor, T. Tohidian and S. Mohebi, Palladium membranes applications in reaction systems for hydrogen separation and purification: A review, Chemical Engineering and Processing: Process Intensification (2017).
8. H. Gao, Y. Lin, Y. Li and B. Zhang, *Ind. Eng. Chem. Res.*, **43**, 6920 (2004).
9. N. Al-Mufachi, N. Rees and R. Steinberger-Wilkens, *Renew. Sust. Energy Rev.*, **47**, 540 (2015).
10. J. D. Way, Palladium/copper alloy composite membranes for high temperature hydrogen separation from coal-derived gas streams, Colorado School of Mines (US) (2003).
11. J. J. Conde, M. Maroño and J. M. Sánchez-Hervás, *Sep. Purif. Rev.*, **46**, 152 (2017).
12. V. Gryaznov, *Platinum Met. Rev.*, **30**, 68 (1986).
13. T. A. Peters, T. Kaleta, M. Stange and R. Bredesen, *J. Membr. Sci.*, **383**, 124 (2011).
14. F. Gallucci, E. Fernandez, P. Corengia and M. van Sint Annaland, *Chem. Eng. Sci.*, **92**, 40 (2013).
15. N. Baronskaya, T. Minyukova, A. Sipatrov, M. Demeshkina, A. Khassin, S. Dimov, S. Kozlov, V. Kuznetsov, V. Y. Terentiev and A. Khristolyubov, *Chem. Eng. J.*, **134**, 195 (2007).
16. C. T. Blaisdell and K. Kammermeyer, *Chem. Eng. Sci.*, **28**, 1249 (1973).
17. A. Basile, L. Paturzo and F. Gallucci, *Catal. Today*, **82**, 275 (2003).
18. F. Gallucci, M. De Falco, S. Tosti, L. Marrelli and A. Basile, *Int. J. Hydrogen Energy*, **33**, 6165 (2008).

19. A. Basile, S. Tosti, G. Capannelli, G. Vitulli, A. Iulianelli, F. Gallucci and E. Drioli, *Catal. Today*, **118**, 237 (2006).

20. V. Piemonte, M. De Falco, B. Favetta and A. Basile, *Int. J. Hydrogen Energy*, **35**, 12609 (2010).

21. C.-H. Kim, J.-Y. Han, H. Lim, D.-W. Kim and S.-K. Ryi, *Korean J. Chem. Eng.*, **34**, 1260 (2017).

22. J. H. Moon and C. H. Lee, *AIChE J.*, **53**, 3125 (2007).

23. J.-H. Moon, J.-H. Bae, Y.-J. Han and C.-H. Lee, *J. Membr. Sci.*, **356**, 58 (2010).

24. X. He, D. R. Nieto, A. Lindbråthen and M. B. Hägg, Membrane System Design for CO2 Capture: From Molecular Modeling to Process Simulation, Process Systems and Materials for CO2 Capture: Modelling, Design, Control and Integration, 10249 (2017).

25. F. Ahmad, K. Lau, S. Lock, S. Rafiq, A. U. Khan and M. Lee, *J. Ind. Eng. Chem.*, **21**, 1246 (2015).

26. Y. Huang, T. C. Merkel and R. W. Baker, *J. Membr. Sci.*, **463**, 33 (2014).

27. A. Caravella, F. Scura, G. Barbieri and E. Drioli, *J. Phys. Chem. B*, **114**, 6033 (2010).

28. D. Mendes, S. Sá, S. Tosti, J. M. Sousa, L. M. Madeira and A. Mendes, *Chem. Eng. Sci.*, **66**, 2356 (2011).

29. F. C. Gielens, H. D. Tong, M. A. G. Vorstman and J. T. F. Keurentjes, *J. Membr. Sci.*, **289**, 15 (2007).

30. T. L. Ward and T. Dao, *J. Membr. Sci.*, **153**, 211 (1999).

31. J.-H. Moon, J.-H. Bae, Y.-S. Bae, J.-T. Chung and C.-H. Lee, *J. Membr. Sci.*, **318**, 45 (2008).

32. L. Yuan, A. Goldbach and H. Xu, *J. Phys. Chem. B*, **111**, 10952 (2007).

33. B. Howard, R. Killmeyer, K. Rothenberger, A. Cugini, B. Morreale, R. Enick and F. Bustamante, *J. Membr. Sci.*, **241**, 207 (2004).

34. A. Goldbach, L. Yuan and H. Xu, *Sep. Purif. Technol.*, **73**, 65 (2010).

35. F. Bustamante, R. Enick, A. Cugini, R. Killmeyer, B. Howard, K. Rothenberger, M. Ciocco, B. Morreale, S. Chattopadhyay and S. Shi, *AIChE J.*, **50**, 1028 (2004).

36. R. K. Helling and J. W. Tester, *Energy Fuels*, **1**, 417 (1987).

37. A. Kulprathipanja, G. O. Alptekin, J. L. Falconer and J. D. Way, *Ind. Eng. Chem. Res.*, **43**, 4188 (2004).

38. A. Basile, G. Chiappetta, S. Tosti and V. Violante, *Sep. Purif. Technol.*, **25**, 549 (2001).

39. S.-W. Lee, J.-S. Park, C.-B. Lee, D.-W. Lee, H. Kim, H. W. Ra, S.-H. Kim and S.-K. Ryi, *Energy*, **66**, 635 (2014).